

## Serological Assessment of Activated Fibroblasts by alpha-Smooth Muscle Actin ( $\alpha$ -SMA): A Noninvasive Biomarker of Activated Fibroblasts in Lung Disorders<sup>1,2</sup>



Signe Holm Nielsen<sup>\*,†</sup>, Nicholas Willumsen<sup>\*</sup>,  
Diana Julie Leeming<sup>\*</sup>, Samuel Joseph Daniels<sup>\*</sup>,  
Susanne Brix<sup>†</sup>, Morten Asser Karsdal<sup>\*</sup>,  
Federica Genovese<sup>\*</sup> and Mette Juul Nielsen<sup>\*</sup>

<sup>\*</sup>Nordic Bioscience A/S, Herlev, Denmark; <sup>†</sup>Disease Systems Immunology, Department of Biotechnology and Biomedicine, Technical University of Denmark, Kgs. Lyngby, Denmark

### Abstract

**OBJECTIVES:** Remodeling of the extracellular matrix (ECM) is a key event in different lung disorders, such as fibrosis and cancer. The most common cell type in the connective tissue is fibroblasts, which transdifferentiate into myofibroblasts upon activation. All myofibroblasts express  $\alpha$ -SMA, which has been found to be upregulated in lung fibrosis and cancer. We evaluated the potential of  $\alpha$ -SMA as a noninvasive biomarker of activated fibroblasts in lung fibrosis and cancer. **METHODS:** A monoclonal antibody was raised against the N-terminal of  $\alpha$ -SMA, and a novel competitive enzyme-linked immunosorbent assay (ELISA) measuring  $\alpha$ -SMA was developed and technically characterized. Levels of  $\alpha$ -SMA were measured in the fibroblast model, “scar-in-a-jar”, and in serum from patients with idiopathic pulmonary fibrosis (IPF), chronic obstructive lung disorder (COPD) and non-small cell lung cancer (NSCLC) belonging to two different cohorts. **RESULTS:** The novel  $\alpha$ -SMA assay was developed and validated as technically robust. Based on the scar-in-a-jar results,  $\alpha$ -SMA was only present in the fibroblasts activated by TGF- $\beta$ . In cohort 1, levels of  $\alpha$ -SMA were significantly higher in IPF, COPD and NSCLC patients compared to healthy controls ( $P = 0.04$ ,  $P = 0.001$  and  $P < 0.0001$ , respectively). The area under the receiver operating characteristics (AUROC) for separation of healthy controls from IPF patients was 0.865, healthy controls from COPD patients was 0.892 and healthy controls from NSCLC patients was 0.983. In cohort 2, levels of  $\alpha$ -SMA were also significantly higher in NSCLC patients compared to healthy controls ( $P = 0$ ) and the AUROC for separating NSCLC and healthy controls was 0.715. **CONCLUSIONS:** In this study we developed and validated a robust competitive ELISA assay targeting the N-terminal of  $\alpha$ -SMA. The level of  $\alpha$ -SMA was upregulated when adding TGF- $\beta$ , indicating that  $\alpha$ -SMA is increased in activated fibroblasts. The level of  $\alpha$ -SMA in circulation was significantly higher in patients with IPF, COPD and NSCLC compared to healthy controls. This assay could potentially be used as a novel noninvasive serological biomarker for lung disorders by providing a surrogate measure of activated fibroblasts.

*Translational Oncology (2019) 12, 368–374*

### Introduction

Extracellular matrix (ECM) remodeling is a key event in diseases such as fibrosis and cancer [1]. Fibroblasts are the most common cell type in connective tissues throughout the body, and the principal source of ECM components of the tissues [2]. The major function of fibroblasts is maintenance and synthesis of new fibrillar collagens to maintain tissue homeostasis. However, upon activation, by either chemical signals that promote proliferation or cellular differentiation, fibroblasts transdifferentiate into myofibroblasts which results in an excessive collagen deposition and tissue remodeling [1,3,4]. Conse-

Address all correspondence to: Signe Holm Nielsen, Nordic Bioscience, Herlev Hovedgade 207, 2730, Herlev, Denmark. E-mail: [shn@nordicbio.com](mailto:shn@nordicbio.com)

<sup>1</sup>Funding Sources: This work was supported by the The Danish Research Foundation (Den Danske Forskningsfond) and The Innovation Foundation (Innovationsfonden).

<sup>2</sup>Conflict of Interest: S. Holm Nielsen, N. Willumsen, D. J. Leeming, M. A. Karsdal, F. Genovese, and M. J. Nielsen are employed at Nordic Bioscience A/S which is a company involved in discovery and development of biochemical biomarkers. M. A. Karsdal, D. J. Leeming, and F. Genovese own stocks in Nordic Bioscience.

Received 1 September 2018; Revised 13 November 2018; Accepted 13 November 2018

© 2018 The Authors. Published by Elsevier Inc. on behalf of Neoplasia Press, Inc. This is an open access article under the CC BY-NC-ND license (<http://creativecommons.org/licenses/by-nc-nd/4.0/>). 1936-5233/19

<https://doi.org/10.1016/j.tranon.2018.11.004>

quently, myofibroblasts are known to be responsible for the increased stiffness of the ECM, as seen in fibroproliferative diseases [5]. In lung tissue there are four possible sources of myofibroblasts; 1) resident fibroblast proliferation and differentiation, 2) circulating fibrocytes attracted to regions of organ injury, 3) endothelial-mesenchymal transition and 4) epithelial-mesenchymal transition [5]. All myofibroblasts express  $\alpha$ -smooth muscle actin ( $\alpha$ -SMA), which is an actin isoform of 42 kDa located in stem- and precursor cells [6].  $\alpha$ -SMA is a well-known and characterized protein used for assessment of activated fibroblasts in several tissues and organs including the lung [7–10], however no serological assay is currently available. The aim of this study was to develop and validate a competitive ELISA targeting  $\alpha$ -SMA and evaluate its association with lung fibroblast activity *in vitro*. In addition, its potential as a noninvasive biomarker was investigated by quantifying the concentration of  $\alpha$ -SMA in serum samples from patients diagnosed with different lung disorders, including idiopathic pulmonary fibrosis (IPF), chronic obstructive pulmonary disease (COPD) and non-small cell lung cancer (NSCLC), in comparison to healthy controls.

**Methods**

**Reagents**

All reagents used for the experiments were standard high quality chemicals from Merck (Whitehouse Station, NJ, USA) and Sigma Aldrich (St. Louis, MO, USA). The synthetic peptides used for production and validation were; I) Coating peptide: Ac-EEEDSTALV-K-Bio, II) Standard peptide: Ac-EEEDSTALV, III) Immunogenic peptide: Ac-EEEDSTALVC-KLH, and IV) Elongated peptide (CEEEDSTALV). They were purchased from Chinese Peptide Company, Beijing, China.

**Generation of Monoclonal Antibodies**

The sequence for  $\alpha$ -SMA <sup>3</sup>EEEDSTALV<sup>11</sup> was aligned between human, mouse, rat, chicken, bovine and rabbit (Figure 1). The first amino acid in  $\alpha$ -SMA is a N-acetylglutamate, hence the Ac-group in the sequence used for this assay. Generation of monoclonal antibodies was performed as previously described [11]. Briefly, production was initiated by subcutaneous immunization of 4- to 5-week-old Balb/C mice with 200  $\mu$ l emulsified antigen and 50  $\mu$ g immunogenic peptide (i.e., KLH-CGG-EEEDSTALV) using Freund's incomplete adjuvant. The immunizations were repeated every second week until stable serum titer levels were reached. The mouse with the highest serum titer was then rested for a month and then boosted intravenously with 50  $\mu$ g immunogenic peptide in 100  $\mu$ l 0.9% NaCl solution three days before isolation of the spleen. The spleen cells were fused with SP2/0 myeloma cells to produce a hybridoma as described by Gefter et al. [12] and cloned in culture dishes using the

**Table 1.**  $\alpha$ -SMA ELISA Technical Validation Data

Technical Validation Test	Result
IC50	3.43 ng/ml
Detection range	0.44-25.5 ng/ml
Intra-assay variation *	8.0%
Inter-assay variation *	13.0%
Dilution recovery of human serum *	99%
Dilution recovery of human urine *	82%
Dilution recovery of rat serum *	84%
Dilution recovery of rat urine *	90%
Analyte recovery 24 h, 4°C/20°C *	102%/97%
Hemoglobin recovery *	86%
Lipemia recovery *	99%
Analyte recovery, 4 freeze/thaw cycles *	97%
Salt recovery, pH 7.0/pH 8.0 †	99%

\* Percentages are reported as mean.

† Average recovery after salt interference.

semisolid medium method. The clones were plated into 96-well microtiter plates for further growth employing the limited dilution method to secure monoclonal growth. Supernatants were screened for reactivity via an indirect ELISA using a streptavidin-coated plate. AC-EEEDSTALV-K-Bio was used as screening peptide, while the free peptide Ac-EEEDSTALV was used to further test for specificity of clones. Supernatant was collected from the hybridoma cells and purified using HiTrap affinity columns (GE Healthcare Life Science, Little Chalfont, Buckinghamshire, UK) according to manufacturer's instructions.

**Ethical Statement**

The production of monoclonal antibodies performed in mice was approved by the National Authority (The Animal Experiments Inspectorate) under approval number 2013-15-2934-00956. All animals were treated according to the guidelines for animal welfare.

**Clone Characterization**

Native reactivity and peptide affinity for the standard peptide were assessed using human serum and urine purchased from a commercial supplier (Valley Biomedical, VA 22602, USA). Antibody specificity was tested in a preliminary assay using deselection and elongated peptides (i.e., standard peptide with 10 amino acid substitutions and standard peptide with one additional amino acid at the N-terminal). The isotype of the monoclonal antibody was determined by using the Clonotyping System-HRP kit, cat. 5300-05 (Southern Biotech, Birmingham, AL).

**$\alpha$ -SMA ELISA**

The  $\alpha$ -SMA procedure was as follows: A 96-well streptavidin-coated ELISA plate (cat. 11940279 from Roche Diagnostics, Hvidovre, Denmark) was coated with the biotinylated peptide (AC-EEEDSTALV-K-Bio), dissolved in assay buffer (50 mM Tris-BTB, 2

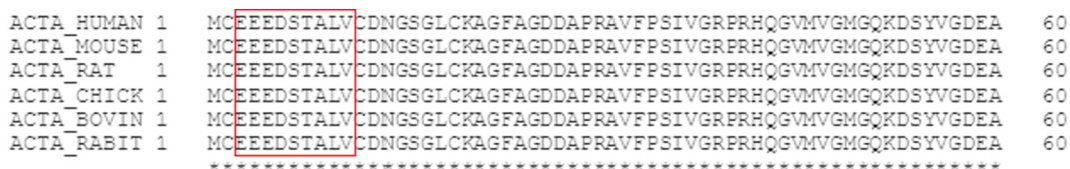


**Figure 1.** Alignment of the targeted  $\alpha$ -SMA sequence in human, mouse, rat, chicken, bovine, and rabbit species (red box). The alignment was performed using Uniprot.

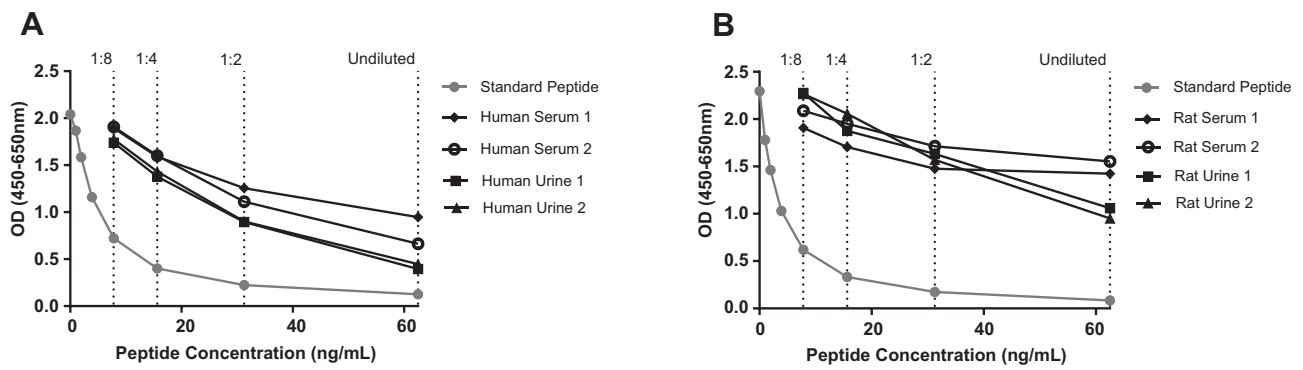


**Figure 2.** Standard curve and native reactivity. A typical standard curve and native reactivity against human serum and urine (A) and rat (B) serum and urine diluted 1:8 for the  $\alpha$ -SMA assay, as indicated. Signals are shown as optical density (OD) at 450 nm, subtracting the background at 650 nm, as a function of standard peptide concentration.

g NaCl/l, pH 8.0), incubated for 30 minutes at 20°C in the dark with 300 rpm shaking, and subsequently washed in washing buffer (20 mM Tris, 50 mM NaCl, pH 7.2). Thereafter, 20  $\mu$ l of peptide calibrator or sample was added to appropriate wells, followed by 100  $\mu$ l of the purified monoclonal antibody diluted in assay buffer, and the plate was incubated for 1 hour at 20°C with 300 rpm shaking and subsequently washed in washing buffer. One hundred microliters of secondary horseradish peroxidase-labeled antibody Peroxidase-AffiniPure Rabbit Anti-Mouse IgG (Cat. 315-035-045, Jackson ImmunoResearch, West Grove, PA) was diluted 1:5000 in assay buffer and incubated for 1 hour at 20°C in the dark with 300 rpm shaking and subsequently washed in washing buffer. Finally, 100  $\mu$ l tetramethylbenzidine (Kem-En-Tec cat. 438OH) was added, and the plate was incubated for 15 minutes at 20°C in the dark with 300 rpm shaking. In order to stop the reaction, 100  $\mu$ l of stopping solution (1% H<sub>2</sub>SO<sub>4</sub>) was added, and the plate was analyzed in the ELISA reader at 450 nm with 650 nm as the reference (SpectraMax M; Molecular Devices, San Jose, CA). A calibration curve was plotted using a four-parametric mathematical fit model. Each ELISA plate included five kit controls to monitor interassay variation. In the final optimized ELISA, all samples were measured within the determined measurement range of the assay, and all samples below lower limit of measurement range (LLMR) were reported as the value of LLMR.

**Technical Evaluation**

All technical evaluations were performed in human serum, human urine, rat serum, and rat urine. Quality control serum and urine samples were used undiluted to determine linearity and calculated as a percentage of recovery of the 100% sample. Lower limit of detection

(LLOD) was calculated as the mean + 3 standard deviation (SD) determined from 21 blank samples (i.e., buffer). Upper limit of detection (ULOD) was determined as the mean - 3\*SD of 10 measurements of the highest point on the standard curve (standard A). The intra- and interassay variation was determined by 10 independent runs of 5 quality control samples, with each run consisting of 2 replicas of the samples. Lower limit of measurement range (LLMR) and upper limit of measurement range (ULMR) were calculated based on the 10 individual standard curves from the intra- and interassay variation. Interference was measured in healthy human serum spiked with hemoglobin (0.08-0.50 mmol/l) or lipids (0.04-0.56 mmol/l). The interference was calculated as the percentage recovery of the analyte in nonspiked serum. Potential salt interference was tested by measuring salt samples with a concentration of 8.14 g/l NaCl at pH 7.0 and pH 8.0. The analyte stability was determined for three healthy human serum samples incubated at either 4°C or 20°C for 2, 4, and 24 hours. The stability of the samples was evaluated by calculating the percentage variation from the sample kept at -20°C (0 hour sample). Furthermore, the analyte stability was determined for three healthy human serum samples exposed to four freeze and thaw cycles. To assess the stability of the analyte, the percentage recovery of the analyte was calculated from the sample that underwent only one freeze/thaw cycle. All sample tests were run as double determinations.

**Biological Validation of  $\alpha$ -SMA**

$\alpha$ -SMA was measured in two different cohorts obtained from the commercial vendor Proteogenex (Culver City, CA). Samples were collected after informed consent and approval by the local

**Table 2.** Patient Demographics of Cohort 1

	Healthy Controls (n = 20)	IPF (n = 10)	COPD (n = 13)	NSCLC (n = 9)	P Value
Age	61.85 (1.95)	73.90 (4.79)	72.15 (3.51)	63.20 (6.70)	<.001
Male, n (%)	10 (50%)	8 (80%)	3 (23.1%)	8 (88.9%)	.005
BMI	26.14 (2.67)	26.22 (1.68)	26.12 (1.90)	N/A	.943
FEV <sub>1</sub> % of predicted value	-	64.50 (1.51)	71.92 (2.96)	-	.0001
FEV <sub>1</sub> /FVC ratio %	-	77.50 (0.85)	56.15 (3.31)	-	<.0001
$\alpha$ -SMA (ng/ml)	7.12	11.92	14.23	19.45	<.0001

Data are presented as mean (SD) unless otherwise stated. Comparison of age, gender, BMI, and  $\alpha$ -SMA levels was performed using Kruskal-Wallis adjusted for Dunn's multiple-comparisons test, while comparison of FEV<sub>1</sub> % of predicted value and FEV<sub>1</sub>/FVC ratio % was calculated using the Mann-Whitney unpaired t test. P values below .05 were considered significant. Abbreviations: BMI, body mass index; FEV<sub>1</sub>, forced expiratory volume in 1 second; FVC, forced vital capacity.

**Table 3.** Patient Demographics of Cohort 2

	Healthy Controls (n = 20)	NSCLC (n = 40)	P Value
Age	61.85 (1.95)	61.93 (2.14)	.593
Male, n (%)	10 (50%)	20 (50%)	1.000
BMI	26.14 (2.67)	25.55 (4.23)	.533
$\alpha$ -SMA (ng/ml)	7.12	10.62	.006

Data are presented as mean (SD) unless otherwise stated. Comparison of age, gender, BMI, and  $\alpha$ -SMA levels was performed using a Mann-Whitney *t* test. *P* values below .05 were considered significant.

Ethics Committee and in compliance with the Helsinki Declaration of 1975.

Cohort 1 included patients diagnosed with IPF (*n* = 10), COPD (*n* = 13), NSCLC (*n* = 9) and colonoscopy-negative controls (*n* = 20) with no symptomatic or chronic disease. Patient demographics are shown in Table 2. Cohort 2 included patients diagnosed with NSCLC in cancer stage I (*n* = 10), II (*n* = 10), III (*n* = 10), and IV (*n* = 10) together with colonoscopy-negative controls (*n* = 20) with no symptomatic or chronic disease. Patient demographics of this cohort are shown in Table 3.

### Scar-in-a-Jar (SiaJ) Model

Primary lung fibroblasts (Lonza, Basel, Switzerland) were cultured in DMEM culture medium supplemented with 10% fetal bovine serum (FBS) and 1% penicillin/streptomycin (P/S) at 37°C and 5% CO<sub>2</sub> and grown until confluency, after which the cells were lifted from the culture flask by trypsinization and counted using a hemocytometer. Fibroblasts were seeded into the wells of a 48-well plate at a density of 30,000 cells/well. Twenty-four hours prior to initiation of the experiment, the cells were serum starved and cultured in DMEM containing 0.4% FBS and 1% P/S. All subsequent media changes used DMEM containing 0.4% FBS and 1% P/S. For the experimental phase, similar to Chen et al. (2009) [13], the cells were cultured in DMEM containing 0.4% FBS, 1% P/S, 225 mg/ml Ficoll 70, 150 mg/ml Ficoll 400 (both Sigma-Aldrich, St. Louis, MO), and 1% ascorbic acid (Wako Chemicals, Neuss, Germany) for 14 days. Media were freshly prepared and changed every 3-4 days. The cells were stimulated with either 1 ng/ml TGF- $\beta$  (R&D Systems, Minneapolis, MN) or vehicle. To ensure cell viability at the start of the experiment and at the termination, the AlamarBlue assay was carried out according to manufacturer’s instructions (Thermo Fisher,

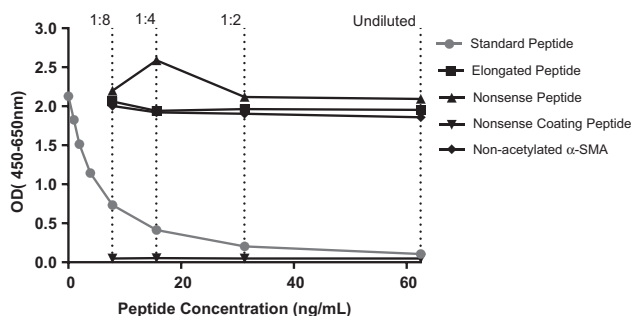


**Figure 3.** Assay specificity. Reactivity to the standard peptide (Ac-EEEDSTALV), the elongated peptide (CEEEEDSTALV), nonsense peptide (PGEILGHVPG), and nonacetylated  $\alpha$ -SMA (EEEDSTALV) was tested for the  $\alpha$ -SMA assay. The background signal from the system was tested using a nonsense coating peptide (Biotin-PGEILGHVPG). Signals are shown as optical density (OD) at 450, subtracting the background 650 nm, as a function of standard peptide concentration.

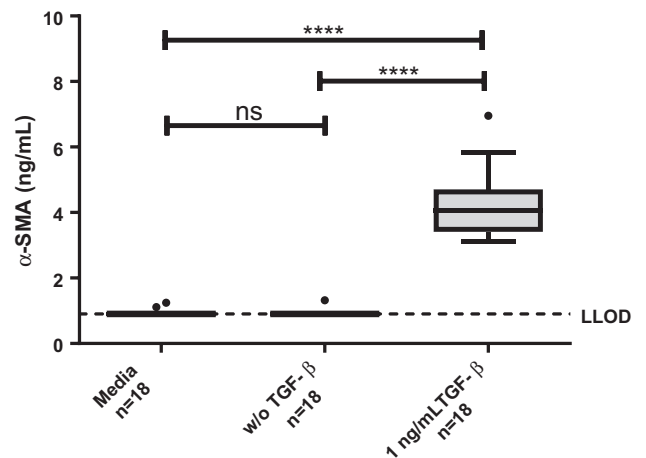


**Figure 4.**  $\alpha$ -SMA in the SiaJ model.  $\alpha$ -SMA was assessed in supernatant of media (background, *n* = 18), cells w/o addition of TGF- $\beta$  (*n* = 18), and cells with 1 ng/ml TGF- $\beta$ . Data are presented as Tukey boxplots, and lower limit of detection of the assay is marked with a dotted line. Significance levels: ns = no significance.

Hvidovre, Denmark). The supernatants were collected after each media change and stored for biomarker assessment at -20°C.

### Western Blotting

Protein concentration of the cell culture supernatant from the SiaJ experiment was determined by Pierce BCA Protein Assay Kit (cat. #23225, Thermo Fisher), and 10  $\mu$ g protein was loaded to a 4%-12% Bis-Tris Gel (cat. #NP0322box, Invitrogen) and separated by SDS-PAGE. Proteins were then transferred onto a nitrocellulose membrane. The membrane was blocked with 5% skim milk powder in TBS-T buffer and incubated at room temperature for 1 hour. The membranes were incubated with 1  $\mu$ g/ml primary  $\alpha$ -SMA antibody at 4°C overnight followed by three washes with TBS-T buffer. The membrane was then incubated in the secondary peroxidase conjugated antibody (1:5000) followed by three times wash with TBS-T. Finally, the results were visualized with ECL detection system (cat. #RPN2109, Amersham Pharmacia).

### Statistical Analysis

Characteristics of the cohorts are presented as a number (frequency) and percentage for categorical variables and mean (SD) for continuous variables. Statistical differences for categorical were assessed using a Kruskal-Wallis test (nonparametric) for cohort 1 and a Mann Whitney *t* test in cohort 2. Results are shown as Tukey boxplots. The diagnostic power of  $\alpha$ -SMA was investigated by the area under the receiver operating characteristics (AUROC) curve. For all statistical analysis performed, a *P* value below .05 was considered significant. Asterisks indicate the following: \**P* < 0.05; \*\**P* < 0.01. Statistical analysis and graphs were performed using GraphPad Prism version 7 (GraphPad Software, Inc., La Jolla, CA).

## Results

### Selection of Peptide Target and Characterization of Antibody Clones

The monoclonal antibody with the best native reactivity, peptide affinity, and stability for the assay was chosen from the antibody-producing clones generated after fusion between mouse spleen cells

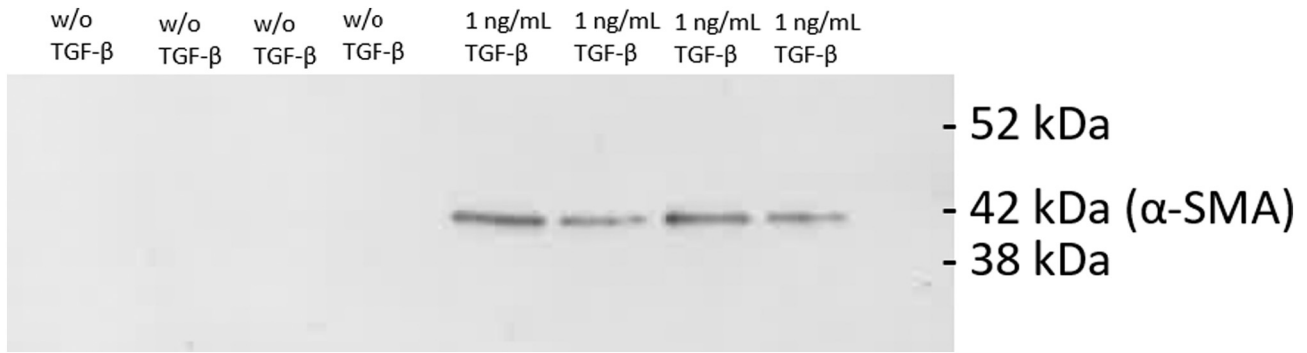


**Figure 5.** Western blot showing the specific bands of  $\alpha$ -SMA in supernatant from the SiaJ model. Lane 1-4: Supernatant from four replicates from the SiaJ model without addition of TGF- $\beta$ . Lane 5-8: Supernatant from four replicates from the SiaJ model with addition of 1 ng/ml TGF- $\beta$ . Bands were observed at 42 kDa for the supernatants with addition of 1 ng/ml TGF- $\beta$ , corresponding to the molecular weight of  $\alpha$ -SMA.

and myeloma cells. Based on reactivity, we selected the antibody clone NB552-2A11. Since the different proteins from the actin family are closely related, three deselection peptides (Ac-DEDETTALV, Ac-EEETTALV, and K-EEEDSTALV) were included during clone selection to ensure specificity towards the  $\alpha$ -SMA sequence.

### Technical Evaluation

A complete technical validation was performed to evaluate the newly developed  $\alpha$ -SMA ELISA. A summary of the technical validation can be found in Table 1. The measurement range (LLMR to ULMR) of the assay was determined to be 0.44-25.5 ng/ml. The intra- and intervariation was 8.0% and 13%, respectively, based on 10 independent assays. Linearity of the human samples was observed from undiluted to eight-fold dilution for human serum, human urine, rat serum, and rat urine (Figure 2). Hemoglobin, lipids, and salt did not interfere with measurements of the  $\alpha$ -SMA analyte in serum or urine. The stability of the analyte was acceptable both during prolonged storage of human serum samples at 4°C and 20°C (102% and 97%, respectively) and during four freeze/thaw cycles (97%).

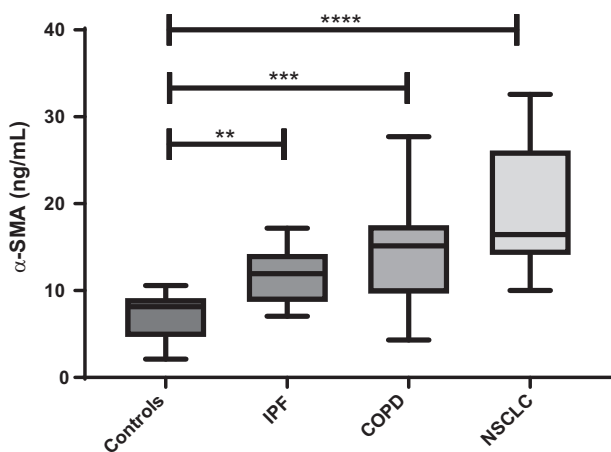


**Figure 6.** Results from cohort 1. Serum  $\alpha$ -SMA levels were assessed in healthy controls ( $n = 20$ ) and in patients with IPF ( $n = 10$ ), COPD ( $n = 13$ ), and NSCLC ( $n = 9$ ). Data were analyzed using a Kruskal-Wallis test adjusted for Dunn's multiple-comparisons test. Data are presented as Tukey boxplots. Significance levels: \*\* $P < .01$ , \*\*\* $P < .001$ , and \*\*\*\* $P < .0001$ .

### Assay Characterization

The analytes detected by the  $\alpha$ -SMA ELISA were characterized by testing reactivity towards synthetic peptides. The assay did not show any reactivity towards an elongated peptide (CEEEDSTALV) or a nonsense peptide (PGEILGHVPG) (Figure 3). No background signal was detected against a nonsense coating peptide (Biotin-PGEILGHVPG), indicating specificity of the antibody. The specificity towards the acetylated  $\alpha$ -SMA was further characterized by measurement of nonacetylated  $\alpha$ -SMA (EEEDSTALV), which showed no reactivity.

### Biological and Clinical Evaluation of the $\alpha$ -SMA Assay

The  $\alpha$ -SMA assay was measured in the SiaJ model and showed to be upregulated by addition of TGF- $\beta$ , indicating that  $\alpha$ -SMA is increased in fibroblasts activated by TGF- $\beta$  (Figure 4). This was furthermore confirmed by Western blot analysis, where  $\alpha$ -SMA only was detected in the supernatants where TGF- $\beta$  was added (Figure 5).

Furthermore, the  $\alpha$ -SMA assay was measured in serum from patients with different lung disorders from two independent cohorts, which will be described as cohort 1 and cohort 2.

Cohort 1 consisted of healthy controls and patients diagnosed with IPF, COPD, and NSCLC. Here, patients with IPF, COPD, and NSCLC were significantly elevated compared to healthy controls ( $P = .04$ ,  $P = .001$ , and  $P < .0001$ , respectively) (Figure 6). No significant difference was observed between IPF patients, COPD patients, and NSCLC patients, indicating that  $\alpha$ -SMA may play an active role in disease. The diagnostic power (AUROC) of  $\alpha$ -SMA for a patient suffering from IPF compared to healthy controls was 0.865 (95% CI = 0.71-1.01,  $P = .0013$ , Figure 7A), COPD compared to healthy controls was 0.892 (95% CI = 0.77-1.02,  $P = .0002$ , Figure 7B), and NSCLC to healthy controls was 0.983 (95% CI = 0.94-1.02,  $P < .0001$ , Figure 7C).

In cohort 2,  $\alpha$ -SMA was measured in samples from healthy controls and patients with NSCLC. Here,  $\alpha$ -SMA was significantly elevated in patients with NSCLC compared to healthy controls ( $P = .006$ ) (Figure 8A), and showed an AUROC of 0.715 (95% CI = 0.58-0.85,  $P = .007$ , Figure 8B). Thus indicating that  $\alpha$ -SMA may be a potential serological biomarker for lung disorders.

### Discussion

In this study, we developed and characterized a competitive ELISA for the detection of  $\alpha$ -SMA using a monoclonal antibody detecting the

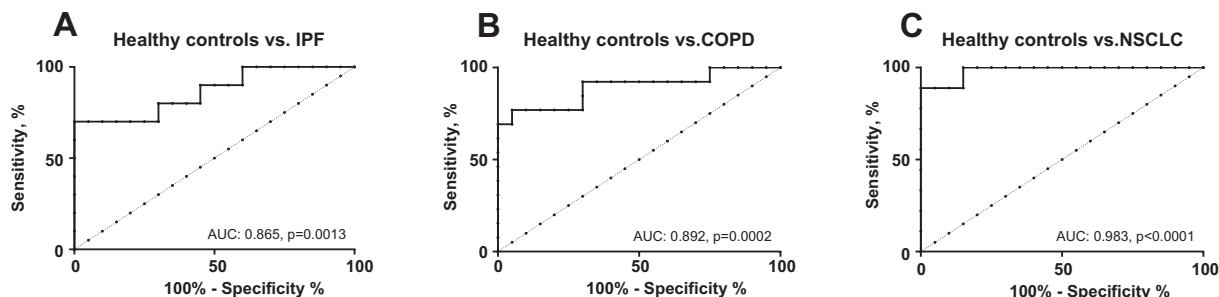


**Figure 7.** ROC curves. ROC curve analysis was used to evaluate the ability of  $\alpha$ -SMA to discriminate between (A) healthy controls and IPF patients, (B) healthy controls and COPD patients and, (C) healthy controls and NSCLC patients.

N-terminal of  $\alpha$ -SMA. The main findings for this study were as follows: 1) the development of a technical robust and specific assay towards the  $\alpha$ -SMA sequence Ac-EEEDSTALV; 2)  $\alpha$ -SMA was detectable in human and rat serum and urine; 3)  $\alpha$ -SMA was significantly elevated in TGF- $\beta$  stimulated fibroblast (the SiaJ model); and 4) the fragment was significantly elevated in patients with IPF, COPD, and NSCLC compared to healthy controls. To our knowledge, this is the first study to show that  $\alpha$ -SMA can be measured noninvasively in supernatant and serum with biological relevance in patients with different lung disorders.

The  $\alpha$ -SMA ELISA is characterized as technically robust and accurate assay showing a dilution recovery, interference, and stability tests within the accepted range of  $\pm 20\%$ . The inter- and intravariation was furthermore accepted with values of 8% and 13%, respectively, and the measurement ranged from 0.44 to 25.5 ng/ml. The assay was further evaluated as specific towards the acetylated N-terminal site of  $\alpha$ -SMA at amino acid position 3 since the first amino acid in  $\alpha$ -SMA consists of an N-acetylglutamate, hence the Ac-group in the sequence used for this assay.

We hypothesized that  $\alpha$ -SMA is a protein that is expressed on the cell surface of fibroblasts and reflects activated fibroblasts in different lung disorders, including fibrotic tissue. Fibroblasts are also found in the tumor microenvironment, where the myofibroblast [or so-called

cancer-associated fibroblast (CAF)] has been shown to be the most abundant stromal cell type. There are several studies supporting the prognostic potential of quantifying  $\alpha$ -SMA assay in relation to lung cancer. In a study evaluating  $\alpha$ -SMA gene expression in tumors from 263 patients with primary lung adenocarcinomas, the patients with high  $\alpha$ -SMA expression presented with enhanced distant metastasis and poor prognosis [14]. Another study revealed that lung CAFs expressed more  $\alpha$ -SMA and had greater contractile capacity than cells from tumor-free lung [15], similar to what is seen in lung fibrosis [9]. Moreover, when compared to normal fibroblast, lung CAFs have also been shown to express higher levels of  $\alpha$ -SMA and promote cellular invasion and differentiation of the lung employed in 3D co-culture, suggesting protumorigenic effects of  $\alpha$ -SMA-positive CAFs [16,17]. The current prognostic potential of  $\alpha$ -SMA has been evaluated by histological assessment of a biopsy. The novel developed assay  $\alpha$ -SMA provides the possibility of a serological assessment of activated fibroblasts and could therefore potentially be used as a noninvasive biomarker for lung disorders.

Similar to  $\alpha$ -SMA, another actin filament that is pathologically relevant and that has shown to be overexpressed in lung cancer tissue is vimentin [18]. Like  $\alpha$ -SMA, vimentin is regarded as a canonical marker for the epithelial-to-mesenchymal transition [19]. Similar to the  $\alpha$ -SMA presented here, our research group has previously shown

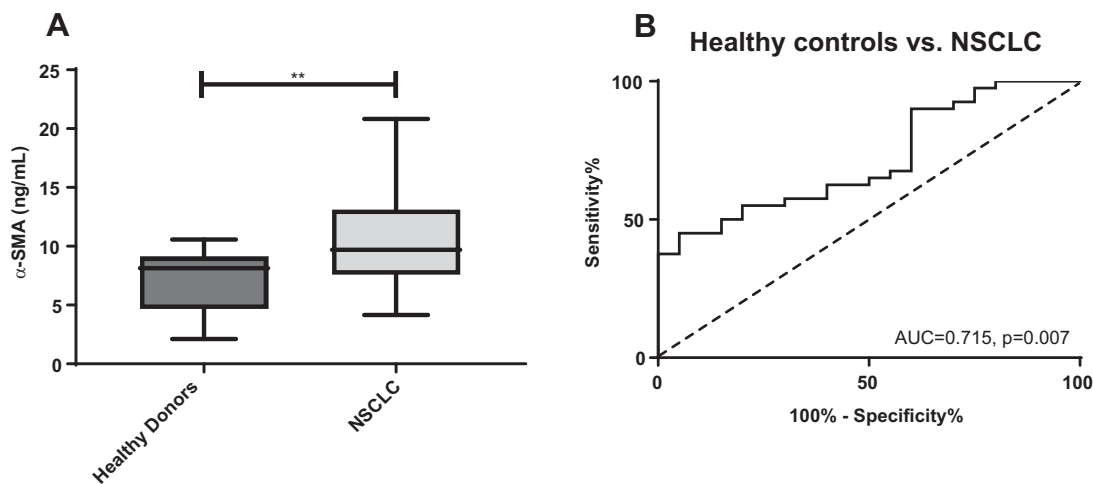


**Figure 8.** Results from cohort 2. (A) Serum  $\alpha$ -SMA levels were assessed in healthy controls ( $n = 20$ ) and NSCLC patients ( $n = 40$ ). Data were analyzed using a Mann Whitney  $t$  test. Data are presented as Tukey boxplots. Significance levels: \*\* $P < .01$ . (B) ROC curve analysis was used to evaluate the ability of  $\alpha$ -SMA to discriminate between healthy controls and NSCLC patients in cohort 2.

that a specific posttranslational modified fragment of vimentin (VICM) was highly elevated in lung cancer patients compared to healthy controls and other cancer types [20]. Clearly, this supports the notion that intracellular proteins/actin filaments are released to the circulation, albeit the exact underlying mechanisms require further investigations. Still, for  $\alpha$ -SMA, the present *in vitro* findings clearly indicate that this release may be associated with TGF- $\beta$  signaling — the most prominent cytokine for induction of fibrogenesis [21]. Interestingly, the NH<sub>2</sub>-terminal sequence of  $\alpha$ -SMA (Ac-EEED), which is the target of the novel  $\alpha$ -SMA assay, is delivered to cultured myofibroblast in the form of a fusion peptide with a cell penetrating sequence; it inhibits their contractile activity [22], suggesting a feedback mechanism on the contractile capacity of activated fibroblast.

One limitation of this study includes the relatively small population size and its cross-sectional design. Only limited data were available from the two cohorts. Still, we were able to find the same trend in  $\alpha$ -SMA in both cohorts. However, whether  $\alpha$ -SMA can be used as a diagnostic, and maybe a prognostic biomarker, needs to be evaluated in larger, prospective cohorts.

## Conclusion

In conclusion, we have developed a specific technically robust ELISA assay for  $\alpha$ -SMA, which may be used for detection of activated fibroblasts in lung disorders. Furthermore, this assay shows promise as a novel noninvasive serological biomarker potential for lung disorders, providing a surrogate measure of activated fibroblasts.

## Acknowledgements

We would like to thank laboratory technician Maiken Helmudt Larsen for help during the initial steps of assay development.

## References

- [1] Karsdal MA, Nielsen MJ, Sand JM, Henriksen K, Genovese F, and Bay-Jensen A-C, et al (2013). Extracellular matrix remodeling: the common denominator in connective tissue diseases possibilities for evaluation and current understanding of the matrix as more than a passive architecture, but a key player in tissue failure. *Assay Drug Dev Technol* **11**, 70–92.
- [2] Kendall RT and Feghali-Bostwick CA (2014). Fibroblasts in fibrosis: novel roles and mediators. *Front. Pharmacol.* [Internet], 5. *Frontiers Media SA*; 2014 123 [cited 2018 Jun 13], Available from: <http://www.ncbi.nlm.nih.gov/pubmed/24904424>.
- [3] King TE, Pardo A, and Selman M (2011). Idiopathic pulmonary fibrosis. *Lancet* (London, England) [Internet], 378. Elsevier; 2011 1949–1961 [cited 2018 Jun 13], Available from: <http://www.ncbi.nlm.nih.gov/pubmed/21719092>.
- [4] Pardo A and Selman M (2016). Lung fibroblasts, aging, and idiopathic pulmonary fibrosis. *Ann. Am. Thorac. Soc.* [Internet], 13. American Thoracic Society; 2016 S417–S421 [cited 2018 Jun 13], Available from: <http://www.atsjournals.org/doi/10.1513/AnnalsATS.201605-341AW>.
- [5] Lomas NJ, Watts KL, Akram KM, Forsyth NR, and Spiteri MA (2012). Idiopathic pulmonary fibrosis: immunohistochemical analysis provides fresh insights into lung tissue remodelling with implications for novel prognostic markers. *Int. J. Clin. Exp. Pathol.* [Internet], 5. e-Century Publishing Corporation; 2012 58–71 [cited 2018 Jun 13]; Available from <http://www.ncbi.nlm.nih.gov/pubmed/22295148>.
- [6] Maher TM, Wells AU, and Laurent GJ (2007). Idiopathic pulmonary fibrosis: multiple causes and multiple mechanisms? *Eur. Respir. J.* [Internet], European Respiratory Society; 2007. p. 835–839 [cited 2018 Jun 13]; Available from: <http://www.ncbi.nlm.nih.gov/pubmed/17978154>.
- [7] Ina K, Kitamura H, Tatsukawa S, and Fujikura Y (2011). Significance of  $\alpha$ -SMA in myofibroblasts emerging in renal tubulointerstitial fibrosis. *Histol Histopathol* **26**, 855–866 [Internet, cited 2018 Jun 13, Available from: <http://www.ncbi.nlm.nih.gov/pubmed/21630215>].
- [8] Carpino G, Morini S, Ginanni Corradini S, Franchitto A, Merli M, and Siciliano M, et al (2005). Alpha-SMA expression in hepatic stellate cells and quantitative analysis of hepatic fibrosis in cirrhosis and in recurrent chronic hepatitis after liver transplantation. *Dig Liver Dis* **37**, 349–356 [Internet, cited 2014 Feb 13, Available from: <http://www.ncbi.nlm.nih.gov/pubmed/15843085>].
- [9] Zhang HY, Gharaee-Kermani M, Zhang K, Karmioli S, and Phan SH (1996). Lung fibroblast alpha-smooth muscle actin expression and contractile phenotype in bleomycin-induced pulmonary fibrosis. *Am J Pathol* **148**, 527–537 [Internet, cited 2018 Jun 13, Available from: <http://www.ncbi.nlm.nih.gov/pubmed/8579115>].
- [10] Lee HW, Park YM, Lee SJ, Cho HJ, Kim D-H, and Lee J-I, et al (2013). Alpha-smooth muscle actin (ACTA2) is required for metastatic potential of human lung adenocarcinoma. *Clin Cancer Res* **19**, 5879–5889 [Internet, cited 2014 Sep 2, Available from: <http://www.ncbi.nlm.nih.gov/pubmed/23995859>].
- [11] Leeming DJ, Nielsen MJ, Dai Y, Veidal SS, Vassiliadis E, and Zhang C, et al (2012). Enzyme-linked immunosorbent serum assay specific for the 7S domain of collagen type IV (P4NP 7S): a marker related to the extracellular matrix remodeling during liver fibrogenesis. *Hepatology Res* **42**, 482–493.
- [12] Gefter ML, Margulies DH, and Scharff MD (1977). A simple method for polyethylene glycol-promoted hybridization of mouse myeloma cells. *Somatic Cell Genet* **3**, 231–236 [Internet, Available from: <http://www.ncbi.nlm.nih.gov/pubmed/605383>].
- [13] Chen C, Peng Y, Wang Z, Fish P, Kaar J, and Koepsel R, et al (2009). The Scar-in-a-Jar: studying potential antifibrotic compounds from the epigenetic to extracellular level in a single well. *Br J Pharmacol* **158**, 1196–1209 [Internet, cited 2018 Aug 9, Available from: <http://www.ncbi.nlm.nih.gov/pubmed/19785660>].
- [14] Lee HW, Park YM, Lee SJ, Cho HJ, Kim D-H, and Lee J-I, et al (2013). Alpha-smooth muscle actin (ACTA2) is required for metastatic potential of human lung adenocarcinoma. *Clin Cancer Res* **19**, 5879–5889.
- [15] Karvonen HM, Lehtonen ST, Sormunen RT, Lappi-Blanco E, Sködl CM, and Kaarteenoaho RL (2014). Lung cancer-associated myofibroblasts reveal distinctive ultrastructure and function. *J. Thorac. Oncol.*, 9. Elsevier; 2014 664–674.
- [16] Horie M, Saito A, Mikami Y, Ohshima M, Morishita Y, and Nakajima J, et al (2012). Characterization of human lung cancer-associated fibroblasts in three-dimensional in vitro co-culture model. *Biochem. Biophys. Res. Commun.*, 423. Academic Press; 2012 158–163.
- [17] Arena S, Salati M, Sorgentoni G, Barbisan F, and Orciani M (2018). Characterization of tumor-derived mesenchymal stem cells potentially differentiating into cancer-associated fibroblasts in lung cancer. *Clin Transl Oncol.* **12**, 1582–1591
- [18] Pelosi G, Melotti F, Cavazza A, Rossi G, Maisonneuve P, and Graziano P, et al (2012). A modified vimentin histological score helps recognize pulmonary sarcomatoid carcinoma in small biopsy samples. *Anticancer Res*, 32. Milan, Italy: Department of Pathology and Laboratory Medicine, Fondazione IRCCS National Cancer Institute; 2012 1463–1473 [giuseppe.pelosi@unimi.it].
- [19] Satelli A and Li S (2011). Vimentin in cancer and its potential as a molecular target for cancer therapy. *Cell Mol Life Sci* **68**, 3033–3046.
- [20] Willumsen N, Bager CL, Leeming DJ, Smith V, Christiansen C, and Karsdal MA, et al (2014). Serum biomarkers reflecting specific tumor tissue remodeling processes are valuable diagnostic tools for lung cancer. *Cancer Med* **3**, 1136–1145 [Internet, cited 2014 Nov 5, Available from: <http://www.ncbi.nlm.nih.gov/pubmed/25044252>].
- [21] Meng X, Nikolic-Paterson DJ, and Lan HY (2016). TGF- $\beta$ : the master regulator of fibrosis. *Nat Rev Nephrol* **12**, 325–338.
- [22] Hinze B, Gabbiani G, and Chaponnier C (2002). The NH<sub>2</sub>-terminal peptide of  $\alpha$ -smooth muscle actin inhibits force generation by the myofibroblast in vitro and in vivo. *J Cell Biol* **157**, 657–663.